BMC Cancer

RESEARCH Open Access

Hypermethylated RASAL1's promotive role in chemoresistance and tumorigenesis of choriocarcinoma was regulated by TET2 but not DNMTs

Xianling Zeng[1*], Ruifang An[2], Ruixia Guo[1] and Han Li[2]

Abstract

Background Patients with choriocarcinoma (CC) accompanying chemoresistance conventionally present a poor prognosis. Whether ras protein activator like-1 (RASAL1) functions as a tumor promoter or suppressor depends on tumor types. However, the role of RASAL1 in process of chemoresistance of CC and underlying molecular mechanism remain elusive.

Methods The expression pattern of RASAL1 in CC cells and tissues was measured using Western blotting, immunohistochemistry and qRT-PCR. Cell viability and proliferative ability were assessed by MTT assay, Tunnel assay and flow cytometric analysis. Additionally, the stemness was evaluated by the colony formation and tumor sphere formation. Methotrexate (MTX) was applied to exam the chemosensitivity of CC cells.

Results The expression of RASAL1 was reduced both at the protein and mRNA levels in CC tissues and cells compared to hydatidiform mole (HM) and invasive mole (IM). Loss of RASAL1 was attributed to its promoter hypermethylation and could be restored by 5-Aza. Knock-down of RASAL1 promoted the viability, proliferative potential, stemness and EMT phenotype of JEG-3 cells. However, induced overexpression of RASAL1 by 5-Aza significantly prohibited cell proliferation and stemness potential of the JAR cell. Additionally, the xenograft model indicated that knockdown of RASAL1 led to a remarkable increase of tumor volume and weight in comparison with its counterpart. Moreover, the stimulatory activity brought by decrease of RASAL1 could be deprived by β-catenin inhibitor XAV 939, yet the suppressive activity resulted from its promoter demethylation could be rescued by β-catenin activator BML-284, indicating that function of RASAL1 depends on β-catenin. Besides, the co-immunoprecipitation assay confirmed the physical binding between RASAL1 and β-catenin. Further investigations showed hypermethylated RASAL1 was regulated by TET2 but not DNMTs.

Conclusion Taken together, the present data elucidated that reduced RASAL1 through its promoter hypermethylation regulated by TET2 promoted the tumorigenicity and chemoresistance of CC via modulating β-catenin both in vitro and in vivo.

*Correspondence:
Xianling Zeng
zxl902x@163.com

Full list of author information is available at the end of the article

Keywords RASAL1, Choriocarcinoma, Chemoresistance, TET2

Introduction

Choriocarcinoma (CC) is the most common malignant gestational trophoblast neoplasia (GTN), characterized by abnormal trophoblastic hyperplasia and associated with high mortality [1, 2]. It arises from any type of gestational events, including hydatidiform mole (HM), abortion, ectopic pregnancy, as well as term delivery [3]. CC is vulnerable to develop early metastasis, affecting lung, liver, brain, etc [1, 4]. Chemotherapy is the mainstay of treatments. The complete remission of single-agent chemotherapy can reach above 80% among patients with low risk of stage I-III [5]. One study showed that 25–30% of low-risk (FIGO score<7) patients would develop resistance or experiment excessive toxicity exerted by initial single-agent chemotherapy [6]. When it comes to patients with a FIGO score of 5–6, the proportion could reach 70–80%. Eventually, they have to be resorted to multi-agent chemotherapy which brings pernicious toxicities. The complete response rate induced by the etoposide, methotrexate, dactinomycin, cyclophosphamide, vincristine (EMA-CO) regimen among high-risk (FIGO score≥7) GTN patients can reach 71–78%. But when it comes to metastatic diseases, the survival rate is only 50–60% [7]. Recently, PD1/PDL-1 immunotherapy has been introduced into the treatment of GTN, dramatically improving the prognosis, but high cost and potential safety risks limits its clinic applications [6, 8, 9]. Therefore, it is imperative to explore new promising strategies.

Chemoresistance is a major culprit contributing to the poor prognosis of patients with CC. Studies have demonstrated that cancer stemness is a crucial factor associated with chemoresistance and is becoming a promising target for the treatment of cancers. However, the exact regulatory molecular mechanism in CC has not been completely elucidated.

Cancer stem cells (CSCs) are a particular subpopulation of cancer cells, endowed with stem-like properties such as pluripotency, differentiation capacity and self-renewal, playing an extremely important role in driving drug resistance, resulting in a poor prognosis [10–15]. Epigenetic alterations during neoplasia are the prominent causes of the arising of CSCs [11, 16]. Studies of various solid tumors suggested that increased Sox2, Nanog and OCT4 could motivate stemness and induce drug resistance. Epithelial-mesenchymal transition (EMT) activation can also promote the emergence of CSCs [17]. EMT is a highly dynamic process of losing apical-basal polarity, allowing cells to transform into a spindle-shaped mesenchymal morphology and further to gain increased motility [18]. EMT enables tumor cells to acquire enhanced stemness and increased resistance to various therapeutic strategies, leading to cancer progression [19, 20]. Accumulating evidence supports the linkage between EMT activation and stemness in many tumors although solid mechanisms remain elusive [20, 21].

RAS protein activator like-1 (RASAL1) is a member of the GTPase activating proteins family. It could enhance the intrinsic GTPase activity of Ras proteins and thereby participates in cell differentiation, proliferation and migration. Increasing evidence has verified that RASAL1 was remarkably downregulated in various tumors, such as hepatic cancer [22], gastric carcinoma [23], colorectal carcinomas [24], and so on, implying that RASAL1 was a candidate tumor suppressor gene. On the contrary, RASAL expression was upregulated in thyroid cancer cells in contrast with non-cancer cells [25]. Additionally, patients with reduced RASAL1 could survive longer and less likely to have distant metastasis in oesophagogastric adenocarcinoma [26]. This paradoxical role of RASAL1 in various cancers underlines that whether RASAL1 would act as a cancer suppressor or a promoter is context-dependent.

To gain insight into the effect of RASAL1 on CC, we sought to clarify the contribution of RASAL1 to the progression and chemoresistance. We first explored the expression pattern of RASAL1 in CC cells and tissues, probing potential epigenetic mechanisms of RASAL1 inactivation in CC cells. Next, RASAL1 was artificially downregulated or demethylated through 5-aza-2'-deoxycytidine (5-Aza), so as to measure the cell viability, proliferative ability, stemness and EMT phenotype. In addition, the in vivo function was tested in nude mouse xenograft model. Finally, the inhibitor and activator were applied to investigate the signaling activity.

Methods and materials

Clinical tissues and immunohistochemistry (IHC)

First trimester villi (FTV), HM, invasive mole (IM) and CC were histologically confirmed at the Department of pathology, the First Affiliated Hospital of Xi'an Jiaotong University. Patient consents were written at the first visit for research purposes. Specimens were from patients who received neither chemotherapy nor radiotherapy previously. The sections were deparaffinized, hydrated and subjected to the endogenous enzyme block. After blocking in 5% BSA, they were incubated in primary antibodies (RASAL1: ab214321, β-catenin: ab32572, Bcl2: ab182858, Oct4: ab181557). Subsequently, they were incubated with secondary antibodies, followed by staining with a diaminobenzidine (DAB) kit and sealing of the sections with Gill's II hematoxylin. Results were assigned into four categories (0, negative; 1–4, weak; 5–8,

moderate; 9–12, strong) according to the calculation of the staining intensity (0, none; 1, weak; 2, intermediate; 3, strong) multiply the percentage of positive cells (0, 0–5%; 1, 6–25%; 2, 26–50%; 3, 51–75%; 4, 76–100%).

Cell culture

HTR-8 and CC cells (JEG-3 and JAR) were obtained from the American Type Culture Collection. HTR-8 cells were cultured in RPMI-1640 medium and JEG-3 and JAR cells were cultured in Dulbecco's modified Eagle's medium (DMEM). Cells were maintained in the culture media supplemented with 10% fetal bovine serum at 37˚C in an incubator with 5% CO2. 5-Aza-2'-deoxycytidine (5-Aza; ab120842) was added to the culture medium at 5 μM. β-catenin pathway inhibitor, XAV 939 (S1180), was added to the culture medium at 2 μM and the activator, BML-284 (sc222416), was at 5 μM. As an equivalent, the same amount of dimethylsulfoxide (DMSO) was added to the medium.

Plasmid construction and short hairpin RNAs (shRNAs) transfection

ShRNAs were first transfected into 293T cells for packaging. After 48 h, the viral supernatant was collected and used for transduction of JEG-3 cells with X-tremeGENE HP DNA transfection reagents. Sequences of shTET2 were as follows: F1: 5′- GCAGCCACCACAGCCCC AGCA-3′, F2: 5′-TATCCATCATATCAATGCAAT-3′. Sequences of shRASAL1 were as follows: F1: 5′- AACC ATCAAGAAGACTCGCTT-3′, F2: 5′-CCAGCAGAAGC CACCTAAAGG-3′. TET2 overexpressing viral supernatant purchased from GenePharma, was utilized to infect JAR cells in the exitance of 8 μg/ml polybrene. To establish stable clone cell lines, puromycin at the concentration of 1.5 μg/ml was used to select infected cells.

Quantitative real-time polymerase chain reaction (qRT-PCR)

According to the manufacturer's instruction, total RNA was extracted using the TRIzol reagent (Life Technologies) and complementary DNA (cDNA) synthesis was performed using a Transcriptor First-Strand cDNA Synthesis Kit (Life Technologies). PCR was performed using SYBR Green qPCR Master Mix (Bio-Rad). The relative expression level was calculated as $2^{-\Delta\Delta Ct}$ based on the threshold cycle (Ct). Sequences of primers were shown in Supplementary Table S1.

Western blotting

Cells and animal tumors were lysed with RIPA buffer (Beyotime biotechnology) and proteins were quantified using a BCA protein assay kit II (BIO-RAD). Equivalent amount of protein from each sample (20–40 μg) were loaded onto the sodium dodecyl sulfate polyacrylamide gel electrophoresis (SDS-PAGE) gel and transferred onto polyvinylidene fluoride (PVDF) membranes (Merck). Membranes were blocked in tris-buffered saline tween (TBST) at room temperature for an hour. Then the blots were cut because certain proteins have similar molecular weights(e.g., E-cadherin 92kD and β-catenin 100kD) which can easily cause confusion on a full membrane. To mark it more clearly, the white space was used or a corner of the strip was cut off in certain bands. The ban were incubated in primary antibodies (shown in Supplementary Table S2) at overnight 4℃ with gentle shaking, followed by a TBST wash. Afterward, membranes were incubated in secondary antibodies for an hour. Finally, the bands were visualized and quantified.

Cell viability and proliferation assay

Cells at the density of 4×10^3/well were seeded into a 96-well plate. A total of 180 μl fresh media mixed with 20 μl MTT (Sigma) was added to each well instead of old media at the 36th hour of culturing. Then, 150 μl DMSO was added into each well after the media was removed at the fourth hour of incubation. The absorbance at 490 nm was measured using a universal microplate reader after shaking for 10 min.

In term of proliferation assay, as what's described above, the absorbance was tested at 12, 24, 36, 48 and 60 h independently. To determine the effect of RASAL1 on chemoresistance, cells at the density of 5×10^3/well were seeded into a 96-well plate. 5-Aza or methotrexate (MTX) at the density of 5 μM was added into the treated well at 24 h according to the protocol. Then the absorbance was measured when the incubation continued for 36 and 48 h.

Colony formation assay

JEG-3 sublines and JAR cells (1×10^3/well) of the exponential growth phase were seeded into 6-well plates and the incubation with complete medium lasted for 2 weeks. Subsequently, each well was washed with phosphate-buffered saline (PBS), fixed in 4% paraformaldehyde and stained with 0.1% crystalline violet solution.

Flow cytometric analysis

As for cell apoptosis analysis, cells with various treatments were washed with cold PBS and stained using the apoptosis kit. With respect to cell cycle analysis, cells at the density of 1×10^6 /ml were harvested, washed and resuspended in binding buffer using the cell cycle kit. The cell suspension was measured immediately using a flow cytometer following the manufacturer's protocol.

Sphere formation assay

Cells at the density of 1×10^3/well were trypsinized to generate a single cell suspension and then plated onto

24-well ultralow attachment plates (Corning) in serum-free DMEM/F12 supplemented with 10 ng/ml human bFGF, 20 ng/ ml human EGF, 2% B27, 1% N2 and penicillin/streptomycin. The plates were coated with poly-HEMA and dried out before using. Two weeks later, cell colonies were washed with PBS, fixed with 4% formalin, and stained with crystal violet. The number of colonies was quantified under five high power microscopic views (×200).

TUNEL assay

Cells with various treatments were fixed with 4% paraformaldehyde and treated with TritonX-100. Then cells were incubated with TUNEL reaction mixture solution which could mark the apoptotic cells following the protocol. DAPI could mark all the cells.

Bisulfite sequencing

Genomic DNA samples were obtained from HTR-8, and JEG-3 and JAR were purified using DNAzol (Invitrogen). Bisulfite treatment of 2.0 μg genomic DNA of cells was performed using the EpiTect Bisulfite Kit (Qiagen,) according to the manufacturer's instructions. Amplified bisulfate PCR products were subcloned into the TA vector system (Promega Corp.) according to the manufacturer's instructions. Five clones were randomly selected for specific regions of the gene and were sent to Sangon Biotech for sequencing.

Immunofluorescence (IF) staining

Approximately 6×10^3 cells were spotted on poly-D-lysinecoated slides. After 8 h, slides were washed in PBS, fixed in 4% paraformaldehyde and permeabilized with Triton X-100. Then cells were incubated with the primary antibody (β-catenin, 1:100), followed by the second antibody (1:150). The nuclei were counterstained with DAPI.

Tumor xenograft model

We conducted the tumor xenograft model according to the guidelines of the Institutional Animal Care and Use Committee of Xi'an Jiaotong University. JEG-3 cell sublines (5×10^6) suspended into 200 μl serum-free DMEM medium which mixed with Matrigel were subcutaneously injected into both flanks (left: shRASAL1-1, right: vector) of almost 5-week-old female athymic nude mice. When the volume of xenografts arrived at about 1000 mm^3, tumor-bearing mice were intraperitoneally injected with MTX (150 mg/kg) once. After one week, euthanasia was carried out by cervical dislocation after rendering nude mice unconscious with ether. Then the xenografts were harvested, weighed and measured. Tumor volume was calculated as length × $width^2$. A part of individual xenograft was fixed with 4% paraformaldehyde and subsequently used for IHC. The remining tumor was processed for western blotting and PCR.

Co-immunoprecipitation (Co-IP)

Cells were harvested, lysed and supplemented with 50 U/mL benzonase (Novagen), protease and phosphatase inhibitors. The eluted proteins were separated by SDS-PAGE and transferred to a PVDF membrane, incubated with primary antibodies against β-catenin and RASAL1 for 2 h, used for western blotting.

Statistical analysis

Individual assay in this present study was biologically replicated more than three times and all the measurements were performed in triplicate. Data were expressed as the mean ± SD. Two-way ANOVA test was used to examine the statistical difference of data between groups. Kaplan–Meier curve was used to analyze the survival rate, including median survival and progress free survival (PFS). Data were statistically analyzed using GraphPad Prism 5.0. Values of $P<0.05$ were considered statistically significant.

Results

RASAL1 was downregulated through its promoter hypermethylation in CC

Results from IHC of FTV ($n=18$), HM ($n=18$), IM ($n=11$) and CC ($n=11$) tissues manifested that the staining of RASAL1 in CC and IM tissues was weaker than that of HM and FTV ($P0.001$). In addition, the weakest staining was in CC (Fig. 1A-C). The fact that the malignancy of gestational trophoblastic disease (GTD) is becoming more aggressive with the decrease of the expression of RASAL1, suggested that the expression of RASAL1 was related to the malignance of GTD. Besides, the protein expression of RASAL1 in CC cells (JEG-3 and JAR) was lower than that in HTR-8, and the mRNA expression showed the same trend ($P0.001$) (Fig. 1D). Among 11 cases of CC, there were 4 chemoresistant cases and 7 chemosensitive cases. In three out of four cases of chemoresistant CC, the staining of RASAL1 was nearly negative (Fig. 1E). What's more, Kaplan–Meier analysis exhibited patients with low-expressed RASAL1 need more chemotherapy courses than those with high-expressed RASAL1 to achieve complete remission ($P=0.0025$) (Fig. 1F). Further investigations into the clinical features of 22 cases of GTN revealed that there was a significant difference between chemoresistant and chemosensitive patients both in the expression of RASAL1 and FIGO stage ($P<0.05$) (Table 1). Overall, the data hinted that decreased RASAL1 lead to poor prognosis, being associated with the tumorigenicity and chemoresistance of CC.

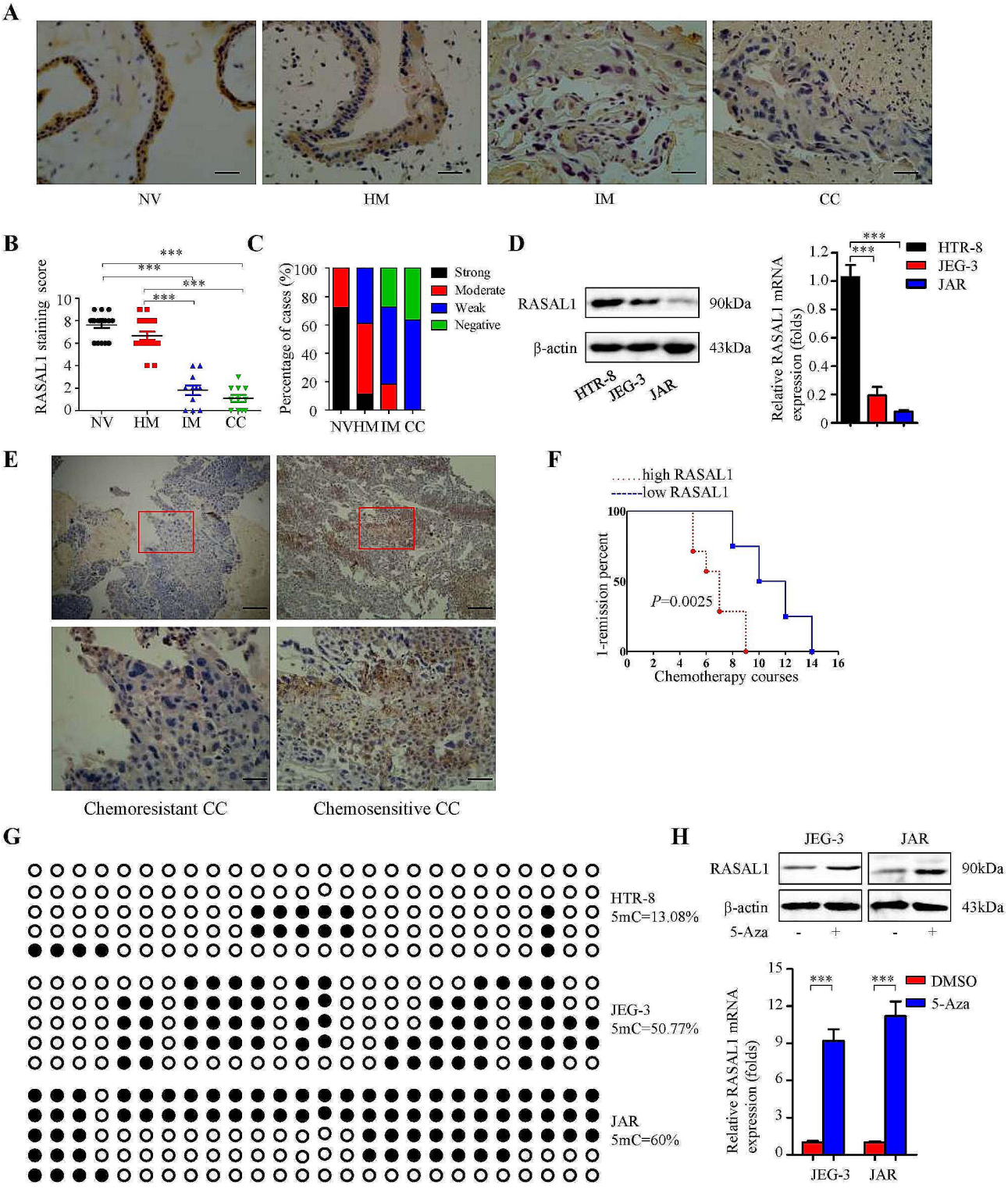

Fig. 1 Decreased RASAL1 was detected in choriocarcinoma tissues and cells. **(A)** IHC staining of RASAL1 in FTV (n = 18), HM (n = 18), IM (n = 11), CC (n = 11). The scale bar is 25μm. **(B)** Quantification analysis, **(C)** and percentage analysis of RASAL1 staining. **(D)** Expression of RASAL1 in HTR-8 and CC cells by qRT-PCR and western blotting. β-actin was used as a loading control. **(E)** IHC staining of RASAL1 in chemoresistant and chemosensitive CC. The scale bar is 25μm. **(F)** Chemotherapeutic remission rate of patients with high or low expression of RASAL1 (n = 7 versus n = 4). **(G)** Individual results for methylation status at each CpG site in HTR-8 and CC cells. Each circle represents a single CpG site. Filled and open circles indicate methylated and unmethylated cytosines. CpG, cytosine-phosphate-guanine. 5mC, cytosine-5′ methylation. **(H)** The expression of RASAL1 in CC cells incubated with 5-Aza for 48 h. ***P<0.001 versus DMSO

Table 1 Analysis of clinical features

Variables	Chemoresistant GTN (*n* = 7)	Chemosensitive GTN (*n* = 15)	HR(95%CI)	*P*
Age (years)				
< 40	2	9	0.267	0.2125
≥ 40	5	6	(0.038–1.852)	
Risk scores				
< 7	2	8	0.35	0.3808
≥ 7	5	7	(0.051–2.407)	
FIGO stages				
I;-II;	1	10	0.083	**0.0337**
III;-IV;	6	5	(0.008–0.895)	
RASAL1 expression				
no	5	2	16.25	**0.0136**
yes	2	13	(1.774-148.846)	

To identify what caused the low expression of RASAL1 in CC, epigenetic modification was considered first and foremost on condition that certain genes were downregulated through CpG hypermethylation of promoters. Hence, we checked the methylation state of RASAL1 gene in CC cells. The finding demonstrated that the methylation frequency was increased in CC cells in comparison with HTR-8 cell, proving that there was a correlation between RASAL1 promoter methylation and decreased RASAL1 (Fig. 1G). To further validate that the loss of RASAL1 was attribute to its DNA promoter hypermethylation, the demethylating agent, 5-Aza, was used to treat CC cells. Results showed that the expression of RASAL1 increased significantly when CC cells were treated with 5-Aza, hinting that the demethylation of RASAL1 gene by 5-Aza could restore its expression in CC cells (Fig. 1H). Comprehensively, we speculated that low-expressed RASAL1 was associated with tumorigenicity and chemoresistance of CC.

Decreased RASAL1 promoted tumorigenesis and chemoresistance in vitro

To deeply figure out the effect of RASAL1 on CC cells, JEG-3 sublines with RASAL1 knockdown were successfully established. The transfected efficiency was verified by western blotting and qRT-PCR (Fig. 2A). Based on the preliminary data, 5-Aza could restore the expression of RASAL1, so 5-Aza was utilized to imitate the JAR overexpressing subline. Results demonstrated that the viability of JEG-3 cell increased after RASAL1 knockdown while the viability of JAR cell with the addition of 5-Aza decreased (Fig. 2B). To determine whether the apoptosis would contribute to the reduction of viability of JAR cells, flow cytometric analysis was performed. Data showed that the percentage of early and late apoptotic cells increased for JAR cell when incubated with 5-Aza, whereas the percentage of apoptotic cells reduced for JEG-3/shRASAL1 sublines (Fig. 2C). The same phenomenon emerged in Tunnel assay which indicated that the proportion of apoptotic JAR cells was greater, yet it was smaller in JEG-3 cells with RASAL1 knockdown (Fig. 2D). On the other hand, cell proliferative potential was facilitated in JEG-3 sublines with RASAL1 knockdown, while it was inhibited in JAR cells treated with 5-Aza (Fig. 2E). It was acknowledged that cell cycle distribution was closely associated with cell proliferation. Therefore, we inferred that RASAL1 may regulate cell proliferation by affecting the cell cycle. As what we expected, the number of JEG-3/shRASAL1 cells entering the S phase was substantially more than that of JEG-3/vector, whereas fewer JAR cells with increased RASAL1 entered S phase (Fig. 2F). These results suggested that reduced RASAL1 in CC cells facilitated its proliferation through affecting cell cycle, in accordance with the expression of protein markers, such as Bcl2, Bax and CyclinD1 (Fig. 2G).

Data showed that EMT could induce chemoresistance in various carcinomas [27, 28]. We initially investigated the state of EMT phenotype in CC cells. The morphology under inverted microscopy manifested that JEG-3 sublines progressively lost their cobblestone epithelial appearance instead of acquiring a spindle-shaped mesenchymal morphology. On the contrary, JAR cells incubated with 5-Aza held together tightly and displayed typical apical basal polarity (Fig. 2H). At the same time, the expression of mesenchymal cell markers (N-cadherin, Vimentin) was stimulated, while the expression of E-cadherin was repressed in JEG-3 sublines with RASAL1 knockdown (Fig. 2G), implying that EMT may involve in the malignancy of CC. Furthermore, the colony formation and tumor sphere formation were stimulated in JEG-3 sublines with RASAL1 knockdown, yet they both were inhibited in JAR cell treated with 5-Aza with great statistical difference (Fig. 2I, J). Accordingly, the expression of protein markers of stemness, like Oct4 and Nanog, elevated obviously in JEG-3/shRASAL1 cells (Fig. 2G). Taken together, decreased RASAL1 activated cell cycle, cancer cell stemness and EMT, thereby further promoting the tumorigenesis and chemoresistance of CC cells.

Decreased RASAL1 promoted tumorigenicity and chemoresistance in vivo

To further confirm whether RASAL1 could regulate tumorigenicity and chemoresistance in vivo, subcutaneous xenografts were established using JEG-3 sublines. Results denoted there was an increase in tumor weight and size of the JEG-3/shRASAL1-1 subline compared with the JEG-3/vector on the 18th day after injection. The tumor weight and size shrunk after intraperitoneal injection of MTX, especially in the JEG-3/vector group

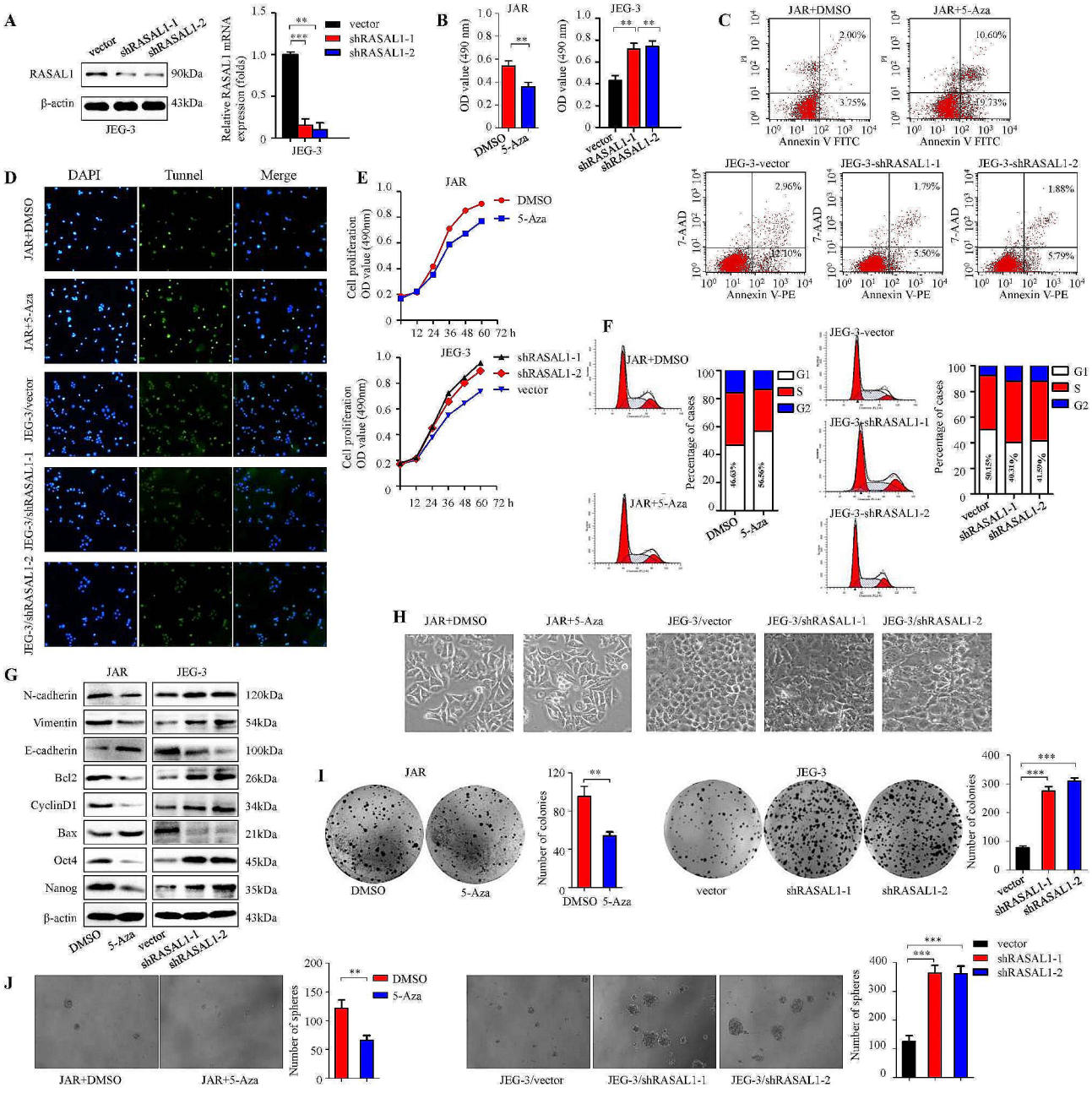

Fig. 2 Downregulated RASAL1 promoted choriocarcinoma cells proliferation. **(A)** Western blotting and qRT-PCR of RASAL1 in JEG-3 sublines. **(B)** Cell viability assay. **(C)** Flow cytometry apoptosis analysis. **(D)** Tunnel assay. **(E)** Cell proliferation experiments. **(F)** Cell cycle analysis. **(G)** Western blotting of protein markers of EMT, proliferation, and stemness. **(H)** Representative images of cell morphology. **(I)** Colony-formation assays. **(J)** Representative images of sphere. $^{**}P < 0.01$, $^{***}P < 0.001$

(Fig. 3A-B). Besides, the expression of stemness-related genes was upregulated in JEG-3/shRASAL1-1 subline (Fig. 3C). Moreover, IHC showed that the staining of β-catenin, Bcl2 and Oct4 in JEG-3/shRASAL1-1 subline was stronger than in JEG-3/vector subline (Fig. 3D). The data suggested suppressed RASAL1 promoted the proliferation and stemness of CC *in vivo.*

Decreased RASAL1 enhanced chemoresistance in CC cells

To probe into whether there was a relationship between reduced RASAL1 and chemoresistance, MTX was added into the culture medium of JAR and JEG-3 sublines at 24 h, and the cell viability was determined by MTT. With the prolonging of time, the cell viability dropped rapidly with the addition of MTX. As for JAR cell, the cell viability of JAR/5-Aza group dropped more drastically than JAR/DMSO group, indicating that increased

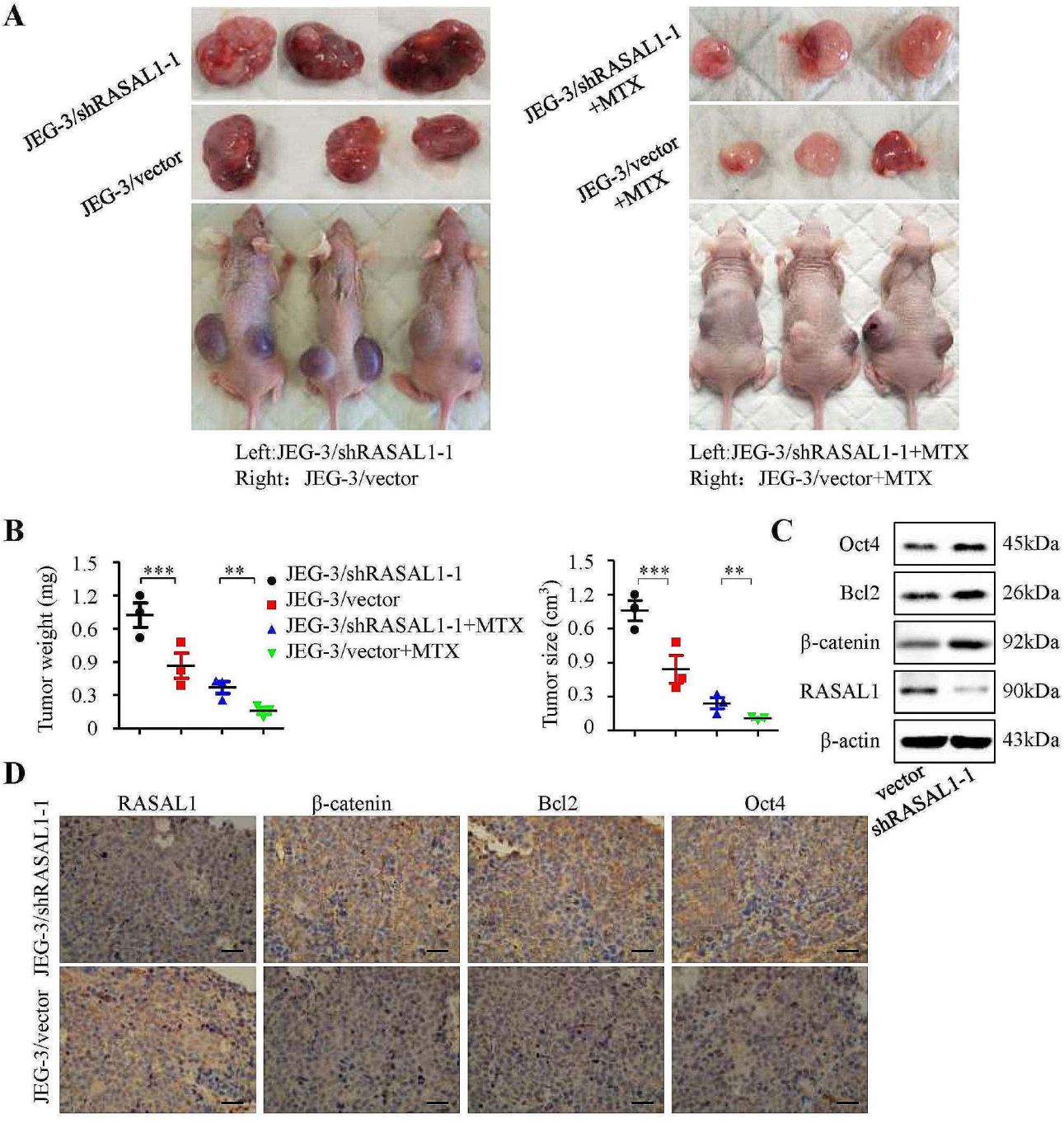

Fig. 3 Effects of RASAL1 in choriocarcinoma's tumorigenicity and proliferation in vivo. **(A)** Representative images of subcutaneous xenografts. **(B)** Tumor growth curve and quantification analysis. Xenograft weight (mg) and volume (cm^3) were measured. **(C)** Western blot analysis of RASAL1, β-catenin, Bcl2 and Oct4. **(D)** IHC staining of xenograft tissues. The scale bar is 40 μm. ***$P < 0.001$

RASAL1 through the demethylation of 5-Aza could boost the chemotherapy sensitivity exerted by MTX. More importantly, JAR cells exposed to the combined application of MTX and Aza have the lowest proliferative potential. In terms of JEG-3 sublines, although the cell activity of JEG-3/shRASL1 decreased remarkably after incubation with MTX, it was still higher than that of JEG-3/vector, suggesting that reduced RASAL1 could enhance the chemoresistance of JEG-3 cells (Fig. 4A). The amount of colony formation in JAR/5-Aza group was less than that of JAR/DMSO group in the existence of MTX, implying that rising RASAL1 made it difficult to endure MTX. On the other hand, the number of colony formation in JEG-3/shRASAL1 was more than that of JEG-3/

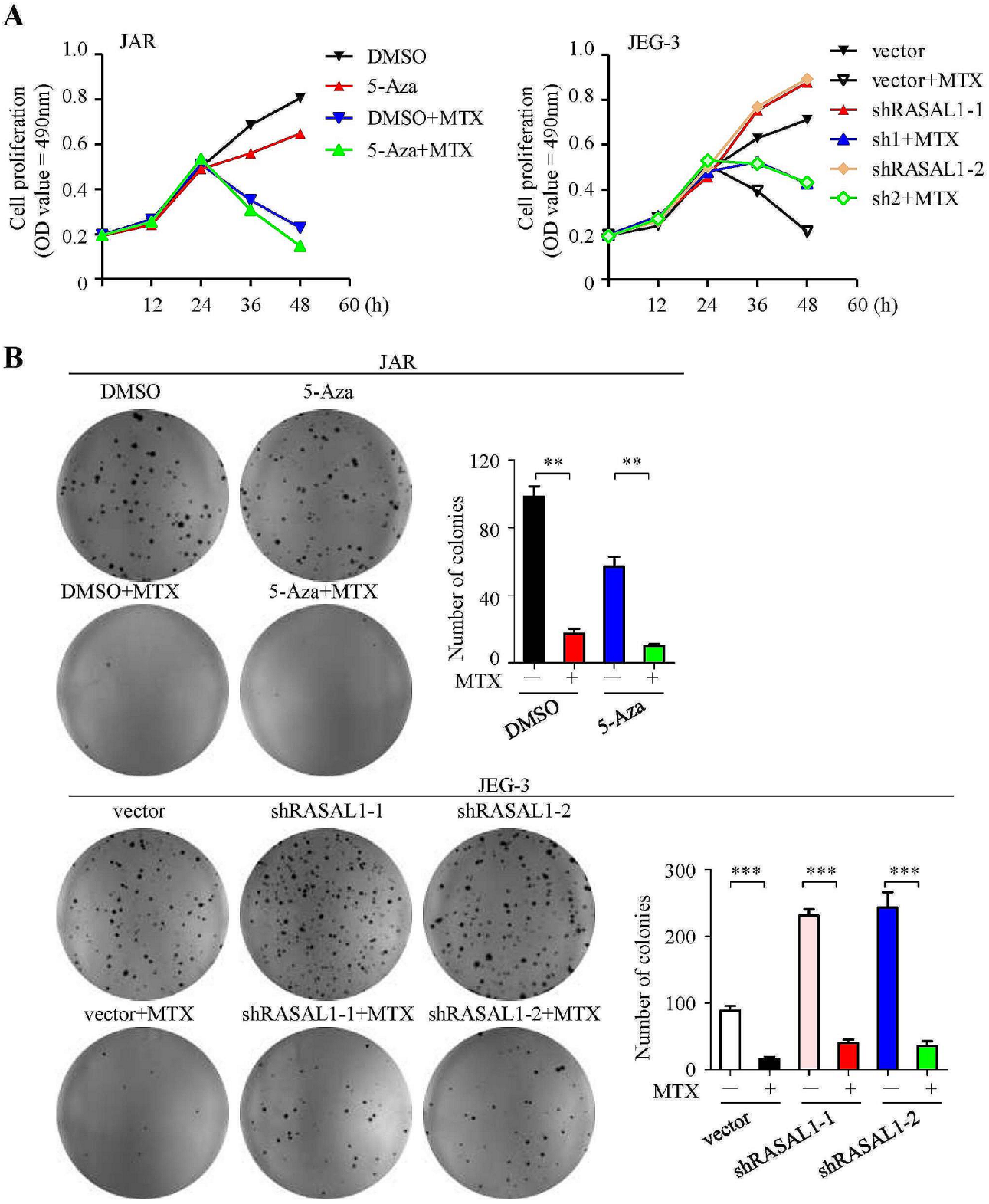

Fig. 4 RASAL1 sensitizes choriocarcinoma cells to MTX. **(A)** Cell proliferative ability. **(B)** Representative images of colony-formation assays in JAR cell and JEG-3 sublines incubated with MTX. $^{**}P < 0.01$, $^{***}P < 0.001$

vector with great statistical difference. This difference is more obvious when the cells are co-cultured with MTX, signifying that depressed RASAL1 enabled JEG-3 cell to acquire chemoresistance (Fig. 4B). Consequently, it can be seen that RASAL1 was involved in the biological process of MTX chemoresistance in CC cells.

RASAL1 modulated tumorigenicity and chemoresistance via β-catenin

Studies found β-catenin was a classical protein, involving in the EMT, stemness and drug resistance in various tumors. In this present study, the IHC staining of β-catenin in JEG-3/shRASAL1-1 cells were significantly higher than that in JEG-3/vector cells, cluing that β-catenin was of supreme importance to the tumorigenicity and chemoresistance of CC. Therefore, we attempted to elucidate the mechanism of RASAL1's promotive role in tumorigenicity and chemoresistance of CC mediated by β-catenin. First and foremost, we undertook to examine the distribution and fluorescence intensity of β-catenin by IF, and results showed fluorescence was mainly in cytoplasm with a little in nucleus in JAR cell treated with DMSO (Fig. 5A above). Meanwhile, there were conspicuous changes in the nuclear retention and fluorescence intensity of β-catenin in JEG-3/shRASAL1 cells in comparison with the JEG-3/vector cells (Fig. 5A below). The data verified that knockdown of RASAL1 lead to the activation of β-catenin, signified by the transfer of β-catenin into the nucleus with large and strong fluorescent spots.

Besides, the expression of p-GSK-3β declined slightly when RASAL1 was upregulated in JAR cells; while the expression increased sharply when RASAL1 was downregulated in JEG-3/shRASAL1 sublines, consistent with the trend of β-catenin (Fig. 5B). To further elucidate this mechanism, the usage of BML-284 in JAR cell demonstrated the activator could rescue the downregulated β-catenin, and inversely, the employment of XAV 939 in JEG-3 sublines showed an inhibition of hyperactivated β-catenin caused by the knockdown of RASAL1(Fig. 5C, D). These data ascertained that RASAL1 could modulate the β-catenin signaling.

Moreover, we aimed to verify the influence of RASAL1 on protein markers associated with cell proliferation, EMT, and cell stemness with the addition of activator or inhibitor. Results indicated that the expression of N-cadherin, Vimentin, and Bcl2, CyclinD1, as well as Oct4, Nanog was inhibited by increased RASAL1, while BML-284 could partially attenuate this inhibitory effect in JAR cells (Fig. 5E). Whereas, the expression was drastically stimulated by downregulated RASAL1, but could be abolished by XAV939 in JEG-3 sublines (Fig. 5F). Taken together, RASAL1 modulated tumorigenicity and chemoresistance through regulating EMT, proliferation and cell stemness via β-catenin.

The stimulatory effect of downregulated RASAL1 on CC cells was regulated by TET2

To further explore the underlying mechanism of the demethylation process of RASAL1 in CC cells, PCR assay was done. Changes of DNMT1, DNMT3a and DNMT3b at mRNA level in HTR8 and CC cells showed no significant difference (Fig. 6A). Simultaneously, changes of TET1 and TET3 were not obvious, but there was statistical significance in TET2 (Fig. 6B), suggesting that the demethylation of RASAL1 of CC cells might be regulated by TET2. In addition, the protein expression of TET2 was less in CC cells than in HTR8 (Fig. 6C). The IHC assay uncovered that the staining of TET2 in CC tissues was weak to negative quantitatively (Fig. 6D-F). What's more, the Kaplan–Meier curve showed patients with high-expressed TET2 owned a longer median survival than the ones with low-expressed TET2 (Fig. 6G). The above results disclosed that TET2 was downregulated in CC cells and tissues, and may be associated with CC's tumorigenicity and chemoresistance.

To ascertain the association between TET2 and RASAL1, we established a stable JAR cell line overexpressing TET2 and JEG-3 cell lines knockdown of TET2, verified by the qRT-PCR and western blotting respectively (Fig. 6H). Concurrently, the methylation frequency of RASAL1 promoter increased in JEG-3/shTET2 cells, while the level of 5-hmC decreased compared to JEG-3/shvector cell. The methylation frequency of RASAL1 promoter in JAR/TET2-OE decreased, while the level of 5-hmC increased in comparison with JAR/vector (Fig. 6L). Besides, the expression of RASAL1 increased in JAR/TET2-OE subline, while the expression decreased in JEG-3/shTET2 sublines, indicating that the methylation process of RASAL1 was regulated by TET2.

The expression of β-catenin, N-cadherin, Bcl2, Oct4, Nanog in JAR/TET2-OE cells decreased sharply, while the expression increased drastically in JEG-3/shTET2-1 cells. Furthermore, the addition of si-RASAL1 placed no impact on the level of TET2, but it rescued the expression of EMT, proliferation and stemness markers which was inhibited by the upregulation of TET2 in JAR/TET2-OE cells. Additionally, 5-Aza deprived the rising momentum of protein markers generated by the downregulation of TET2 in JEG-3/shTET2-1 cells (Fig. 6I). On the other hand, no changes were seen in the containment of TET2 both in JAR cells incubated with 5-Aza and in JEG-3 cells with knockdown of RASAL1. While, the expression of β-catenin showed a changing tread, similar to its active state (Fig. 6J), implying that RASAL1 was one of the downstream targets of TET2. Concurrently, the co-IP assay indicated that there was an interaction between

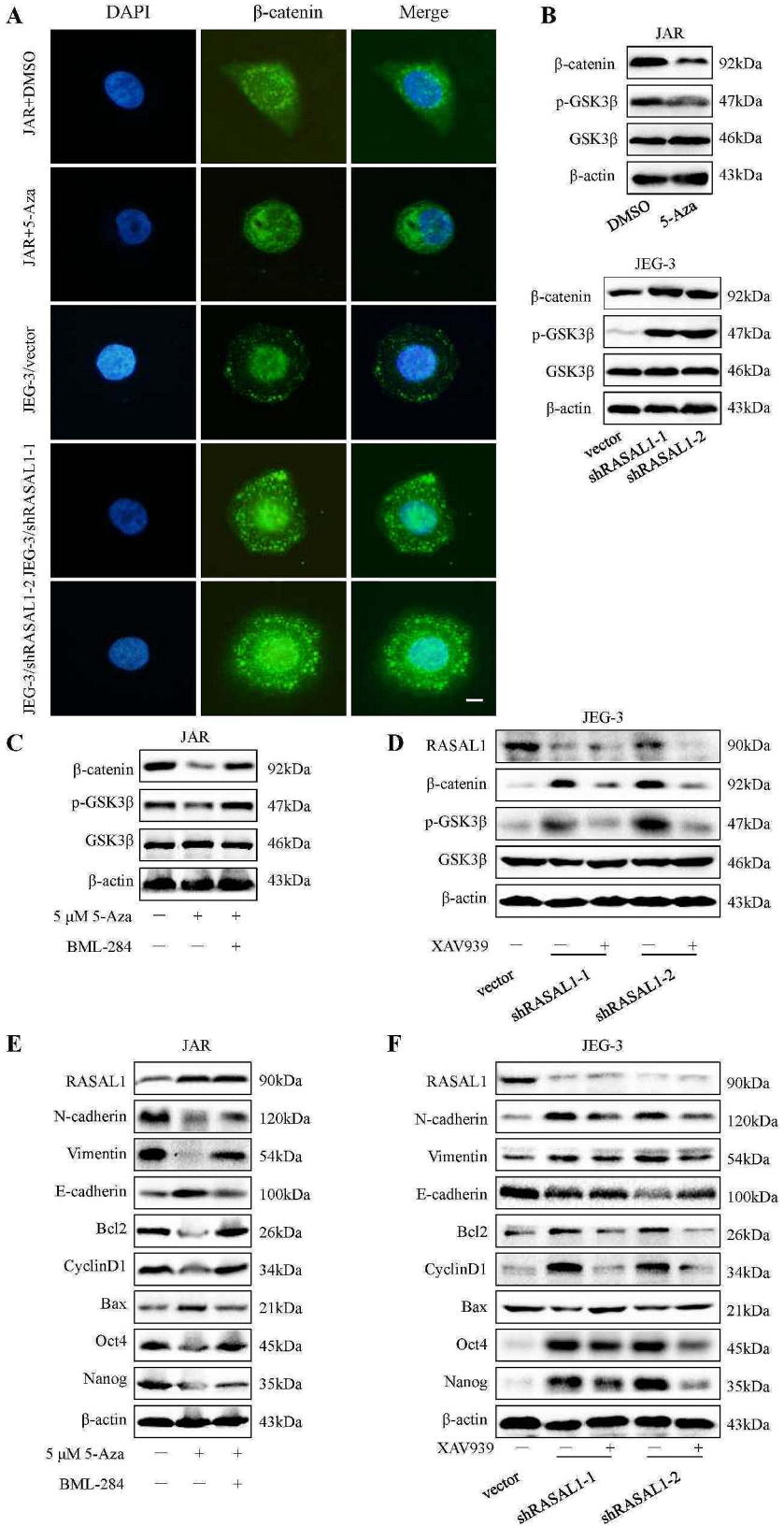

Fig. 5 RASAL1 modulated tumorigenicity and proliferative ability via β-catenin in choriocarcinoma cells. **(A)** IF staining with antibodies against β-catenin (green) and DAPI (nuclei, blue) in JAR cell incubated with 5-Aza and JEG-3 sublines. The scale bar represents 25 μm. (**B**-**C**) Western blotting assay in JAR treated with both 5-Aza and BML-284, **(D)** and in JEG-3 sublines treated with XAV939. **(E)** Expression of protein markers of EMT, proliferation, and stemness in JAR treated with both 5-Aza and BML-284, **(F)** and in JEG-3 sublines treated with XAV939

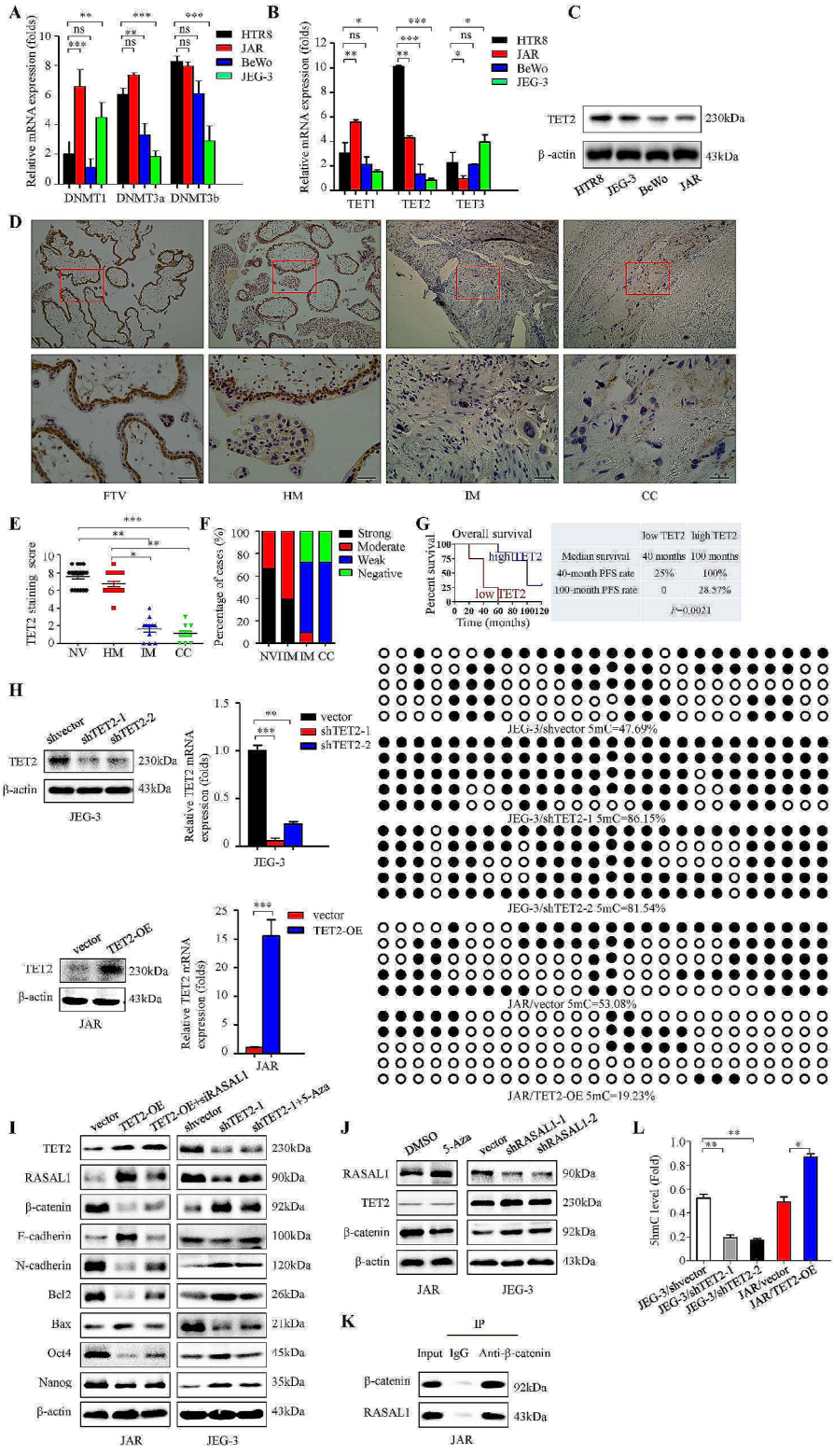

Fig. 6 It's TET2 not DNMTs modulating tumorigenicity via RASAL1 by targeting β-catenin in CC cells. **(A)** Changes of DNMTs, **(B)** and TETs in HTR8 and CC cells. **(C)** Western blotting of TET2 in cells. **(D)** IHC staining of TET2 in FTV ($n = 18$), HM ($n = 18$), IM ($n = 11$), CC ($n = 11$). The scale bar is 25 μm. **(E)** Quantification analysis, **(F)** and percentage analysis of TET2 staining. **(G)** Prognostic data for CC patients with high or low expression of TET2. **(H)** Expression of TET2 and the methylation frequency of RASAL1 promoter in JEG-3 and JAR sublines. **(I)** Expression of RASAL1 and protein markers of EMT, proliferation, and stemness, **(J)** and the expression of TET2, β-catenin in JAR and JEG-3 sublines. **(K)** Co-immunoprecipitation assay of RASAL1 and β-catenin in JAR cells. (L) Global 5-hmC levels in JEG-3 and JAR sublines. *$P < 0.05$, **$P < 0.01$, ***$P < 0.001$

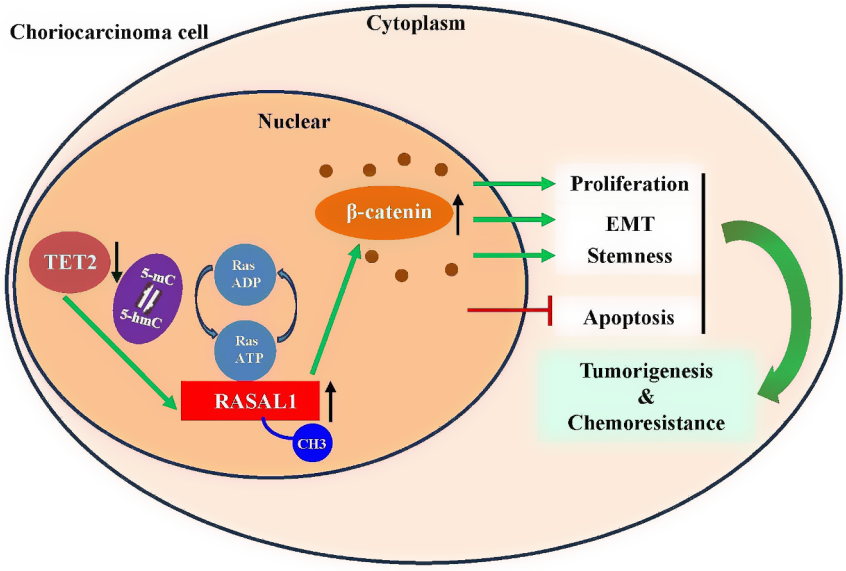

Fig. 7 The proposing schematic of mechanism. Downregulated TET2 in CC cells prevents the demethylation of RASAL1 gene promoter, leads to the increase of methylated RASAL1 and results in the decrease of RASAL1. And then the rising active β-catenin promotes the proliferation, EMT, stemness, and represses apoptosis, and eventually stimulates the tumorigenesis and chemoresistance of CC cells. Black arrow-head represents promotion

β-catenin and RASAL1 (Fig. 6K). Overall, the data demonstrated that downregulated RASAL1 regulated by TET2 could promote tumorigenicity and chemoresistance in CC through β-catenin.

Discussion

CC heavily affects patients' quality of life and brings about huge economic burden [29, 30]. The cure rate for patients scoring 0–1 with single agent treatment is close to 90%, but it drops to 33% for those with a score of 5–6 [8]. It is well recognized that the risk of chemoresistance increases as the score rises, especially for patients at ultra-high risk. They are simultaneously at high risk of early or late death. It was speculated that chemoresistance was the major determinant of treatment failure in CC. Given the increasing rate of resistance to the single agent, multi-agent chemotherapy treatments are administrated to such patients from the outset, exposing more patients to unnecessary toxicity.

Empirical evidence verified that RASAL1 was a suppressor in many tumors, but as of yet, the relationship between RASAL1 and CC has not been unambiguously determined. The present study showed that the expression of RASAL1 was reduced no matter in CC cells or tissues. Deep investigations into the causes of downregulated expression of RASAL1 denoted that its promoter hypermethylation was the culprit and the methyltransferase inhibitor, 5-Aza, could rescue its expression. This was in line with various cancers' states where the epigenetic modification commonly happens and is responsible for the loss of RASAL1. Deficiency of RASAL1 was related to the chemoresistance and lower remission rate of CC patients. Overall, the observation indicated that reduced RASAL1 lead to chemoresistance and malignant progression, supporting the notion that RASAL1 could serve as a valuable biomarker in predicting the prognosis and chemosensitivity in patients with CC.

Much evidence suggested EMT contribute to drug resistance in multiple cancers and may serve as a potential target for overcoming chemoresistance [31, 32]. Many studies showed that EMT transcription factors, like Snail, Slug and Zeb1, were responsible for the resistance to cisplatin-based and oxaliplatin-based chemotherapeutic regimens in kinds of cancers [31, 33, 34]. CSCs possess characteristics associated with EMT, forming the helmet of various tumors [18, 32]. Detailed functional assays in this study for the first time found that downregulated RASAL1 promoted cell viability, proliferative ability, stemness and EMT phenotype in CC, endowed CC cells with unique chemoresistant properties, in consistent with previous researches about other tumors. In particularly, we found that RASAL1 knockdown promoted sphere-formation ability and increased the expression of stemness-related genes which maintain CSC-like properties. Conversely, RASAL1 overexpression repressed the EMT phenotype and stemness. The data confirmed that the regulation of RASAL1 was a major mechanism underlying the chemoresistance of CC.

Convincing evidence hold that cells undergoing EMT conventionally share crucial signaling pathways and drug resistance phenotypes with CSCs [31, 35]. Our forepassed study verified the role of β-catenin in EMT phenotype of CC thoroughly. Therefore, it was speculated that RASAL1 would modulate the stemness and EMT

via β-catenin pathway. In the present study, decreased RASAL1 in CC cells dramatically enhanced the containment of β-catenin, indicating that β-catenin was involving in mediating the chemoresistance, EMT and stemness of CC.

In mammalian cells, DNA methylation is regulated by DNA methyltransferases (DNMTs), including DNMT1, DNMT3a and DNMT3b. Besides, active DNA demethylation is mediated by ten-eleven translocation (TET) proteins. Further investigations into the causes of demethylation of RASAL1 in CC cells showed that the modulatory role of RASAL1 in cells' viability, EMT and stemness was mediated by TET2 but not DNMTs (Fig. 7).

Our findings are of great importance in unraveling new avenues for increasing the chemosensitivity of CC, in the hope of improving prognosis. However, the conclusion may not be suitable for other tumors due to the intertumoral heterogeneity, making the applicable scope difficult to expand. Besides, the translation of this theoretical basic research into clinical applications needs more deep investigations. So future efforts should be focused on consolidating this theory, anticipating to provide fundamental insights into the complex networks that orchestrate EMT, stemness and chemosensitivity of CC.

In conclusion, our data demonstrated that downregulated RASAL1 through its promoter aberrate hypermethylation which was regulated by reduced TET2 promoted the activity of β-catenin, further triggered series of biological behaviors, including promoting proliferation and initiating stemness, and eventually contributed to the carcinogenesis and chemoresistance of CC. Besides, the combination of 5-Aza and MTX could enhance the chemosensitivity of CC. These findings add much more information to our current knowledge about the newly found molecular mechanism underlying CC's chemoresistance, and further provide new opportunities to overcome the limitations of current therapeutic regimens to improve the clinical outcome of patients with CC.

Supplementary Information

The online version contains supplementary material available at https://doi.org/10.1186/s12885-024-12758-w.

Supplementary Material 1

Supplementary Material 2

Supplementary Material 3

Acknowledgements
Not applicable.

Author contributions
Xianling Zeng, Ruifang An and Ruixia Guo: conception and design of the work; Xianling Zeng, Ruifang An and Han Li: acquisition, analysis or interpretation of data; Xianling Zeng: article writing with contributions from other authors. Ruifang An and Ruixia Guo revised the manuscript. All authors approved the final manuscript and agreed to be accountable for the work.

Funding
This study was supported by the National Natural Science Foundation of China (no. 81671491 and no. 81172489) and the Henan Provincial Medical Science and Technology Research Plan Joint Construction Project (no. LHGJ20200313).

Data availability
The datasets used and/or analyzed during the current study are available from the corresponding author on reasonable request.

Declarations

Ethics approval and consent to participate
All animal studies were approved by the Animal Use and Care Committee of Xi'an Jiaotong University. The authors confirmed that all animal experiments were performed in accordance with ARRIVE guidelines (https://arriveguidelines.org). Also, the experiments with human tissues was also approved by the Ethics Committee of the First Affiliated Hospital of Xi'an Jiaotong University. All the methods/study was in accordance with the declaration of Helsinki, and all methods were conducted in accordance with relevant guidelines and regulations. The human tissues from all subjects were obtained with informed consents.

Consent for publication
Not applicable.

Competing interests
The authors declare no competing interests.

Author details
[1]Department of Gynecology, The First Affiliated Hospital of Zhengzhou University, No.1 East Jianshe Road, Zhengzhou, Henan 450052, China
[2]Department of Obstetrics and Gynecology, The First Affiliated Hospital of Xi'an Jiaotong University, Xi'an, Shaanxi 710004, China

Received: 15 November 2023 / Accepted: 2 August 2024
Published online: 08 August 2024

References

1. Kaur B. Pathology of gestational trophoblastic disease (GTD). *Best practice & research Clinical obstetrics & gynaecology* 2021, 74:3–28.
2. Lukinovic N, Malovrh EP, Takac I, Sobocan M, Knez J. Advances in diagnostics and management of gestational trophoblastic disease. Radiol Oncol. 2022;56(4):430–9.
3. Abu-Rustum NR, Yashar CM, Bean S, Bradley K, Campos SM, Chon HS, Chu C, Cohn D, Crispens MA, Damast S, et al. Gestational trophoblastic neoplasia, Version 2.2019, NCCN Clinical Practice guidelines in Oncology. J Natl Compr Cancer Network: JNCCN. 2019;17(11):1374–91.
4. Ngan HYS, Seckl MJ, Berkowitz RS, Xiang Y, Golfier F, Sekharan PK, Lurain JR, Massuger L. Diagnosis and management of gestational trophoblastic disease: 2021 update. Int J Gynaecol Obstet. 2021;155(Suppl 1):86–93.
5. Berkowitz RS, Goldstein DP. Current management of gestational trophoblastic diseases. Gynecol Oncol. 2009;112(3):654–62.
6. Winter MC. Treatment of low-risk gestational trophoblastic neoplasia. Best Pract Res Clin Obstet Gynecol. 2021;74:67–80.
7. Lurain JR. Gestational trophoblastic disease II: classification and management of gestational trophoblastic neoplasia. Am J Obstet Gynecol. 2011;204(1):11–8.
8. Clark JJ, Slater S, Seckl MJ. Treatment of gestational trophoblastic disease in the 2020s. Curr Opin Obstet Gynecol. 2021;33(1):7–12.
9. Ghorani E, Kaur B, Fisher RA, Short D, Joneborg U, Carlson JW, Akarca A, Marafioti T, Quezada SA, Sarwar N, et al. Pembrolizumab is effective for drug-resistant gestational trophoblastic neoplasia. Lancet. 2017;390(10110):2343–5.
10. Caglar HO, Biray Avci C. Alterations of cell cycle genes in cancer: unmasking the role of cancer stem cells. Mol Biol Rep. 2020;47(4):3065–76.
11. Li H, Feng Z, He ML. Lipid metabolism alteration contributes to and maintains the properties of cancer stem cells. Theranostics. 2020;10(16):7053–69.
12. Barbato L, Bocchetti M, Di Biase A, Regad T. Cancer Stem cells and targeting strategies. Cells 2019, 8(8).

13. Thankamony AP, Saxena K, Murali R, Jolly MK, Nair R. Cancer Stem Cell plasticity - A Deadly Deal. Front Mol Biosci. 2020;7:79.
14. Vessoni AT, Filippi-Chiela EC, Lenz G, Batista LFZ. Tumor propagating cells: drivers of tumor plasticity, heterogeneity, and recurrence. Oncogene. 2020;39(10):2055–68.
15. Kharkar PS. Cancer Stem Cell (CSC) inhibitors in Oncology-A Promise for a better therapeutic outcome: state of the art and future perspectives. J Med Chem. 2020;63(24):15279–307.
16. Feinberg AP, Koldobskiy MA, Göndör A. Epigenetic modulators, modifiers and mediators in cancer aetiology and progression. Nat Rev Genet. 2016;17(5):284–99.
17. Ponomarev A, Gilazieva Z, Solovyeva V, Allegrucci C, Rizvanov A. Intrinsic and extrinsic factors impacting Cancer Stemness and Tumor Progression. Cancers (Basel) 2022, 14(4).
18. Dongre A, Weinberg RA. New insights into the mechanisms of epithelial-mesenchymal transition and implications for cancer. Nat Rev Mol Cell Biol. 2019;20(2):69–84.
19. Nieto MA, Huang RY, Jackson RA, Thiery JP. EMT: 2016. Cell. 2016;166(1):21–45.
20. Lu W, Kang Y. Epithelial-mesenchymal plasticity in Cancer Progression and Metastasis. Dev Cell. 2019;49(3):361–74.
21. Ju F, Atyah MM, Horstmann N, Gul S, Vago R, Bruns CJ, Zhao Y, Dong QZ, Ren N. Characteristics of the cancer stem cell niche and therapeutic strategies. Stem Cell Res Ther. 2022;13(1):233.
22. Calvisi DF, Ladu S, Conner EA, Seo D, Hsieh JT, Factor VM, Thorgeirsson SS. Inactivation of ras GTPase-activating proteins promotes unrestrained activity of wild-type Ras in human liver cancer. J Hepatol. 2011;54(2):311–9.
23. Qiao F, Su X, Qiu X, Qian D, Peng X, Chen H, Zhao Z, Fan H. Enforced expression of RASAL1 suppresses cell proliferation and the transformation ability of gastric cancer cells. Oncol Rep. 2012;28(4):1475–81.
24. Ohta M, Seto M, Ijichi H, Miyabayashi K, Kudo Y, Mohri D, Asaoka Y, Tada M, Tanaka Y, Ikenoue T, et al. Decreased expression of the RAS-GTPase activating protein RASAL1 is associated with colorectal tumor progression. Gastroenterology. 2009;136(1):206–16.
25. Liu H, Li Z, Li L, Peng H, Zhang Z. EBP1 suppresses growth, migration, and invasion of thyroid cancer cells through upregulating RASAL expression. Tumour Biology: J Int Soc Oncodevelopmental Biology Med. 2015;36(11):8325–31.
26. Knief J, Reddemann K, Lazar-Karsten P, Herhahn T, Petrova E, Wellner U, Thorns C. Prognostic implications of RASAL1 expression in oesophagogastric adenocarcinoma. J Clin Pathol. 2017;70(3):274–6.
27. Fischer KR, Durrans A, Lee S, Sheng J, Li F, Wong ST, Choi H, El Rayes T, Ryu S, Troeger J, et al. Epithelial-to-mesenchymal transition is not required for lung metastasis but contributes to chemoresistance. Nature. 2015;527(7579):472–6.
28. Zheng X, Carstens JL, Kim J, Scheible M, Kaye J, Sugimoto H, Wu CC, LeBleu VS, Kalluri R. Epithelial-to-mesenchymal transition is dispensable for metastasis but induces chemoresistance in pancreatic cancer. Nature. 2015;527(7579):525–30.
29. Seckl MJ, Sebire NJ, Berkowitz RS. Gestational trophoblastic disease. Lancet. 2010;376(9742):717–29.
30. Lok C, Frijstein M, van Trommel N. Clinical presentation and diagnosis of gestational trophoblastic disease. Best Pract Res Clin Obstet Gynecol. 2021;74:42–52.
31. Singh A, Settleman J. EMT, cancer stem cells and drug resistance: an emerging axis of evil in the war on cancer. Oncogene. 2010;29(34):4741–51.
32. Shibue T, Weinberg RA. EMT, CSCs, and drug resistance: the mechanistic link and clinical implications. Nat Reviews Clin Oncol. 2017;14(10):611–29.
33. Guo W, Keckesova Z, Donaher JL, Shibue T, Tischler V, Reinhardt F, Itzkovitz S, Noske A, Zürrer-Härdi U, Bell G, et al. Slug and Sox9 cooperatively determine the mammary stem cell state. Cell. 2012;148(5):1015–28.
34. Siebzehnrubl FA, Silver DJ, Tugertimur B, Deleyrolle LP, Siebzehnrubl D, Sarkisian MR, Devers KG, Yachnis AT, Kupper MD, Neal D, et al. The ZEB1 pathway links glioblastoma initiation, invasion and chemoresistance. EMBO Mol Med. 2013;5(8):1196–212.
35. Mani SA, Guo W, Liao MJ, Eaton EN, Ayyanan A, Zhou AY, Brooks M, Reinhard F, Zhang CC, Shipitsin M, et al. The epithelial-mesenchymal transition generates cells with properties of stem cells. Cell. 2008;133(4):704–15.

Publisher's Note